*Int. J. Electrochem. Sci.*, 10 **(2015)** 5521 - 5529

International Journal of
ELECTROCHEMICAL
SCIENCE
www.electrochemsci.org

# Electrochemical Properties of Electrodeposited PEDOT Counter Electrode for Dye-sensitized Solar Cells

*Chang Kook Hong*[1], *Hyun Seok Ko*[2], *Eun Mi Han*[1], *Kyung Hee Park*[3,*]

[1]School of Applied Chemical Engineering, Chonnam National University, Gwangju 500-757, Republic of Korea
[2]Department of Advanced & Chemicals, Chonnam National University, Gwangju 700-757, Republic of Korea
[3]The Research Institute of Advanced Engineering Technology, Chosun University, Gwangju 501-759, Korea
[*]E-mail: see0936@chosun.ac.kr

*Received:* 30 March 2015 / *Accepted:* 2 May 2015 / *Published:* 27 May 2015

Poly(3,4-ethylenedioxythiophene) (PEDOT) films were coated on fluorine-doped tin oxide (FTO) conductive glass by electrodeposition and applied as the counter electrode (CE) in dye-sensitized solar cells (DSSCs). Scanning electron microscopy (SEM) revealed the nanofiber-like structure of the PEDOT films. The maximum energy conversion efficiency obtained from the 0.5-μm-thick PEDOT CE was 5.1%, which was almost equivalent to that of the standard Pt CE (5.2%). From electrochemical impedance spectroscopy (EIS) results, the large charge transfer resistance of direct current solar cells was attributed to the formation of unbounded PEDOT chains that minimized the $I_3^-$ reduction rate.

**Keywords:** Electrodeposition, poly(3,4-ethylenedioxythiophene), dye-sensitized solar cells, counter electrode, photovoltaic performance

## 1. INTRODUCTION

The dye-sensitized solar cell (DSSC) has attracted considerable attention in the search for cheap key materials to promote its performance [1,2]. DSSCs consist of three main components: a dye-sensitized nanocrystalline titanium oxide layer on a transparent conductive oxide as a working electrode, $I^-/I_3^-$ redox couple as an electrolyte, and a platinized electrode as a counter electrode (CE). The role of the CE is to collect electrons from the external circuit and reduce $I_3^-$ to $I^-$ in the electrolyte. Usually, a Pt-coated electrode is used as the CE and acts as a reduction catalyst [3-5]. However, as a noble metal Pt is expensive. Also, the slow dissolution of the Pt CE in the corrosive $I_3^-/I^-$ redox

electrolyte deteriorates the long term stabilities of DSSCs. As such, a new substitute for Pt would enable to reduce the cost of DSSCs. A counter electrode desired high conductivity, chemical stability, corrosion resistance against iodides, and a suitable catalyst for the $I_3^-$ reduction [6,7]. Recently, conductive polymers such as poly(3,4-ethylenedioxythiophene:poly(4-styrenesulfonate)) (PEDOT:PSS), polypyrrole (PPy), and polyaniline (PANI) were reported excellent electrocatalytic CE catalysts [8-10].

The most common redox couple is tri-iodide/iodide ($I_3^-/I^-$). $I^-$ is oxidized to $I_3^-$ at the dye (Eq. 1) and $I_3^-$ is reduced to $I^-$ at the cathode (Eq. 2) [11]:

$$3I^- \rightarrow I_3^- + 2e^- \quad (1)$$

$$I_3^- + 2e^- \rightarrow 3I^- \quad (2)$$

PEDOT is known to be a potential alternative to Pt due to its good conductivity, remarkable stability, and a comparatively lower price than Pt [12-14].

In this study, we demonstrate that the development of PEDOT CE has focused on the use of electropolymerized PEDOT, dispersed into a solvent, coated onto a conducting substrate and optimized thickness control for high efficiency. Also, chemically synthesized PEDOT on a conducting fluorine-doped tin oxide (FTO) substrate is used as a CE and the effect on the performance of the DSSCs is investigated.

## 2. EXPERIMENT

### *2.1 Materials and chemicals*

3,4-Ethylenedioxythiophene (EDOT, 97%) and propylene carbonate were purchased from Aldrich. Tetrabutylammonium hexafluorophosphate ($TBAPF_6$, 99.0%, Fluka), acetonitrile ($CH_3CN$, 99.8%), and lithium perchlorate ($LiClO_4$, 99.99%) were purchased from Aldrich. All reagents were of analytical grade and used as received. The aqueous solutions were prepared with double distilled water. High pure nitrogen was used for deaeration. FTO conducting glass (TEC-8) was purchased from Pilkington (USA). Surlyn films of 25 μm thickness were purchased from Solaronix S.A

### *2.2 Prepared PEDOT counter electrode (CE)*

The PEDOT film was deposited on FTO-glass substrates by electropolymerization of EDOT solution under different sweep segments. The electrochemical experiments were carried out with a three-electrode system. The working and counter electrodes were FTO glass and Pt wire, respectively. The reference electrode was Ag/AgCl (sat'd NaCl). The electrochemical measurements were performed on a CHI 660A electrochemical workstation. The thickness of the PEDOT film was controlled by the number of polymerization cycles. The concentration of the monomer solution was

0.1 M dissolved in the electrolyte solution, 0.1 M $TBAPF_6/CH_3CN$. The scan rate of the potential was 50 $mVs^{-1}$. The electrochemical cells were degased by nitrogen bubbling prior to each experiment.

*2.3 DSSC fabrication*

$TiO_2$ paste (DSL 18NR-T, Dyesol) was used to prepare the $TiO_2$ films for the DSSCs. In each case, the $TiO_2$ paste was coated on pre-cleaned FTO glass using a squeeze printing technique, followed by annealing at 450 $^oC$ for 30 min. An approximately 10-μm-thick $TiO_2$ film of area 0.25 $cm^2$ was deposited on the FTO glass substrate. The annealed film was then immersed overnight (ca. 24 h) in a $5\times10^{-4}$ mol/L ethanol solution of $Ru(dcbpy)_2(NCS)_2$ (535-bis TBA, Solaronix), rinsed with anhydrous ethanol and dried. The electrolyte composition was 0.05 M $I_2$ (Aldrich, 99.999%), 0.5 M LiI (Aldrich, 99.9%), 0.3 M 1,2-dimethyl-3-propylimidazolium iodide (Aldrich), and 0.5 M 4-*tert*-butylpyridine (Aldrich, 99%), using 3-methoxypropionitrile (Fluka, 99%) as solvent. The dye-adsorbed $TiO_2$ electrode and CE were assembled into a sealed sandwich-type cell with a gap of a thermoplastic polymer, Surlyn (25 μm).

*2.4 Characterization and measurements*

The film surface morphology and thickness were characterized by field emission scanning electron microscopy (FE-SEM, Hitachi, S-4700). Incident photon-to-current conversion efficiency (IPCE) (PV Measurements, Inc.) was measured as a function of wavelength from 300 nm to 800 nm under irradiation of a dispersed 300W Xe lamp. The catalytic activities of the PEDOT and Pt films were analyzed by cyclic voltammetry (CV) with symmetric platinized FTO glass (or PEDOT)/electrolyte/ platinized FTO glass (or PEDOT) at a scan rate of 50 $mVs^{-1}$. Electrochemical impedance spectroscopy (EIS) was used to analyze the resistance of the electrochemical system. The photovoltaic properties were investigated by measuring the current density-voltage (*J-V*) characteristics under white light irradiation from a 200 W Xenon lamp (K201-LAB50, McScience, Korea) at AM 1.5 G condition. The incident light intensity was 100 $mWcm^{-2}$.

## 3. RESULTS AND DISCUSSION

The polymerization proceeded easily even when low monomer concentrations were used. The polymerization made by potential scanning between -1.5 and 1.5 V in 0.1 M EDOT in acetonitrile containing 0.1 M $TBAPF_6$ is shown in Figure 1(a). Oxidization and polymerization of the monomer commenced from ca. 1.0 V during the first anodic scan. The increasing peak currents from the redox processes of the film with increasing number of deposition cycles indicated a continuous growth of material on the electrode. The peak current increased linearly with increasing scan cycle. The films created during electrodeposition were light blue and darkened with continuing electrodeposition time, as shown in the inset of Figure 1(a). Figure 1(b) shows the CV curves of the resulting PEDOT film in a

monomer-free electrolyte solution. The shape of the CV curve was similar to that reported in the literature [15]. It can be observed that the current increased with increasing deposited cycle number. This can be attributed to thicker layers of PEDOT which increase the conductivity and electrochemical surface area that resulted in a larger area of electrodeposited PEDOT. However, there was the slight shift in the reduction peaks of 4 cycles and current decreased than 3 cycles. This can be explained by thicker PEDOT layer has the slower electron transfer. The PEDOT electrode was made by using the 3-cycle deposited film because the peak current of 3 cycles was higher than that of 2 and 4 cycles.

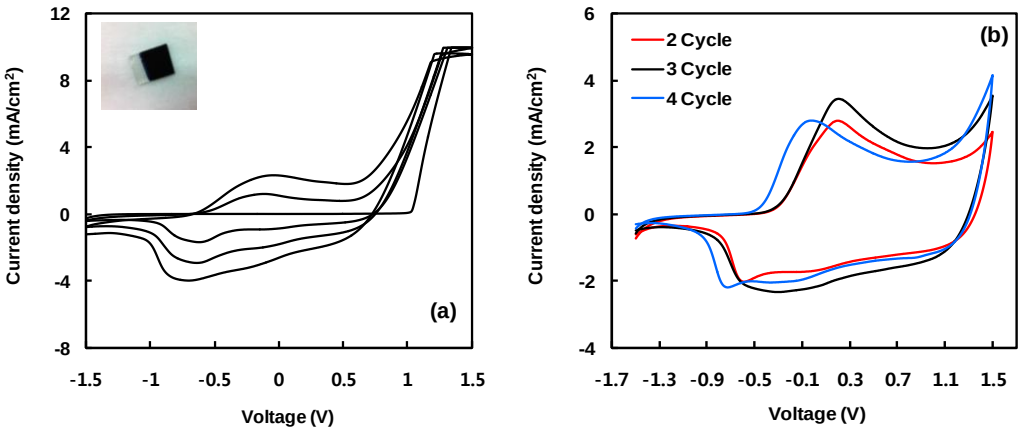


**Figure 1.** (a) Polymerization by potential cycling between -1.5 V and 1.5 V of a 0.1 M EDOT solution in 0.1 M $TBAPF_6/CH_3CN$ at 50 mV $s^{-1}$. (b) Cyclic voltammogram of PEDOT in monomer-free 0.1 M $TBAPF_6/CH_3CN$ solution at 50mV$s^{-1}$.

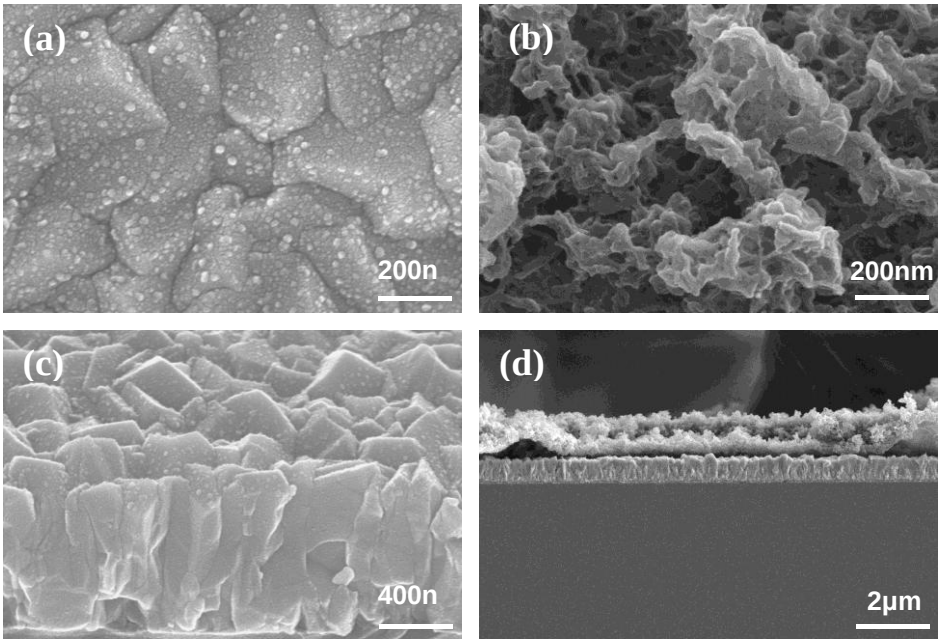


**Figure 2.** SEM images of surface and cross section of the platinized FTO glass electrode (a and c, respectively) and surface and cross section of PEDOT deposited electrode (b and d, respectively).

The surface morphologies of Pt and PEDOT on FTO glass in the SEM images are shown in Figure 2. The Pt particles with a mean size of 10 nm were distributed homogeneously on the surface of the FTO glass. Electropolymerized PEDOT film exhibits a nanofiber-like morphology and is highly porous with a network structure, which dictates its catalytic activity. The porous structure has a high specific surface area and can be regarded as a potential. The porous structure is advantageous for improving the electrocatalytic activity of the $I^-/I_3^-$ redox reaction.

The PEDOT films were characterized through Fourier transform infrared spectroscopy (FT-IR). Figure 3 shows the FT-IR spectra obtained for a PEDOT film sample. Signals at 1512, 1458, and 1392 $cm^{-1}$ were associated with the C=C and C-C bonds in the thiophene ring. The peaks at 871 and 671 $cm^{-1}$ were attributed to the C-S interaction in the thiophene ring, and peaks 1257 through 1049 $cm^{-1}$ corresponded to the ethylenedioxy group [16]. Based on this, it was concluded that PEDOT was the material sampled.

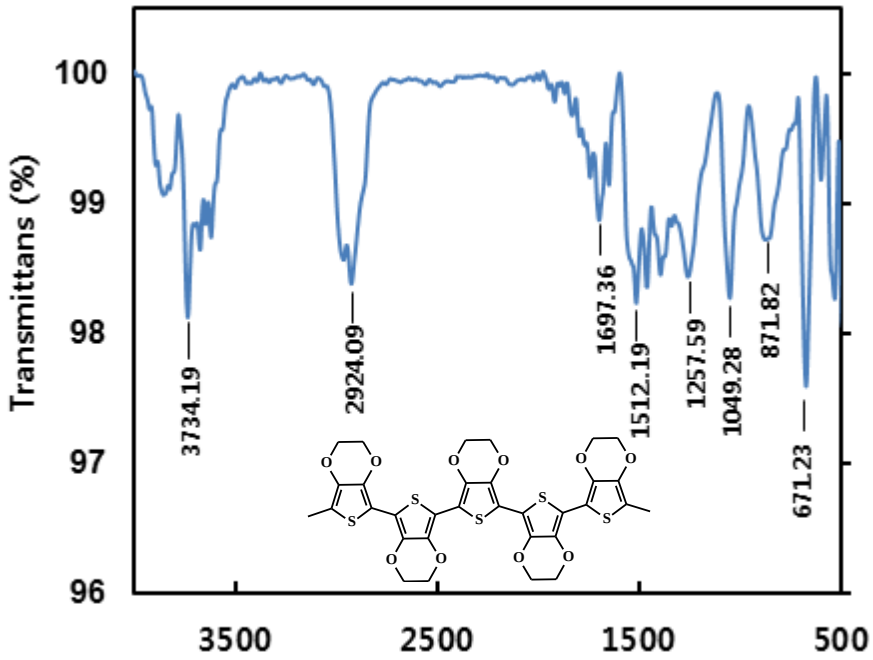


**Figure 3.** FT-IR spectrum and structure of electrode based on PEDOT film**.**

The role of CE is vital to collect electrons from the external circuit and catalyze the $I_3^-$ reduction in the electrolyte. To investigate the electrocatalytic activity of the prepared CE towards the $I^-/I_3^-$ redox reaction was studied by CV measurement. Figure 4 shows CVs of the Pt and PEDOT electrodes at different scan rates in the potential range of -1.5 ~1.5 V. Those on the upper half correspond to oxidation while those in the lower half correspond to the reduction process. The first reduction peak in the CV marked as (I) is due to the reaction: $3I_2 + 2e^- = 2I_3^-$ [17] which is unimportant in the context of DSSC operation. The second peak marked as (II) is due to the reduction of $I_3^-$ by the reaction: $I_3^- + 2e^- = 3I^-$ [18]. This reaction occurs at the CE of a DSSC and is vital for its functioning.

Thus the magnitude of the current density at the second peak (*Ip*) is directly proportional to the ability of the electrode to reduce the $I_3^-$ species. On the other hand, the reduction peak current density of the PEDOT/FTO glass was slightly greater than that of the Pt/FTO glass, due to the high active surface area of PEDOT/FTO. The CV result shows that PEDOT/FTO is more electrochemically active, which indicates a much faster reaction rate on PEDOT. Therefore, PEDOT is expected to substitute the expensive Pt as a promising CE catalyst.

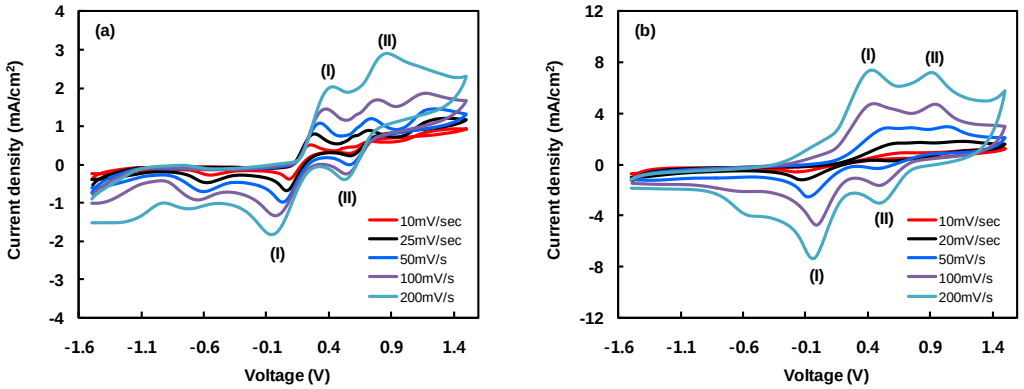


**Figure 4.** The CVs of iodide species on Pt (a) and PEDOT (b) film in acetonitrile solution containing 10 mM LiI, 1 mM $I_2$ and 0.1 M $LiClO_4$ taken at various scan rates ranging from 10 to 200 mV/s.

Electrochemical impedance experiments were performed to estimate the reduction of $I_3^-$ ions on the CE. Fig. 5(a) shows a proposed equivalent circuit model for the Pt or PEDOT DSSC in equilibrium conditions. Fig. 5(b) shows Nyquist plots for the electrochemical cells with Pt and PEDOT films in the frequency range of 0.1 - $10^6$ Hz. Two distinct semicircles are observed for both DSSCs. The semicircles in the higher frequency region (~kHz range) are associated with charge transfer ($R_{ct}$) at the CE/electrolyte interface and those in a 10 – 100 Hz range are related to a charge-transfer process at the $TiO_2$/dye/electrolyte interface. A clear difference is evident in the impedance spectra of the two CEs of the DSSCs. The electron transfer resistance at the CE/electrolyte interface ($R_{ct}$) of PEDOT DSSCs is about 2.3 Ω, which is much lower than that of the Pt DSSCs (~10.2 Ω). Furthermore, two characteristic frequencies were observed in the Bode phase plots (Fig. 5(c)) for the electrochemical cells with Pt and PEDOT electrodes. In the high frequency region, the $R_{ct}$ value of PEDOT appears smaller than that of Pt cell, according to the equation $J_o=RT/nFR_{ct}$, in which R, T, and F are the gas constant, temperature, and Faraday constant, respectively. Therefore, the faster reduction rate of $I_3^-$ ions caused by the increased electrocatalytic activity increased $J_{sc}$ for the PEDOT cell due to the decreased $R_{ct}$. The reduced interface resistance speeded up the interfacial electron transfer, and hence raised the efficiency.

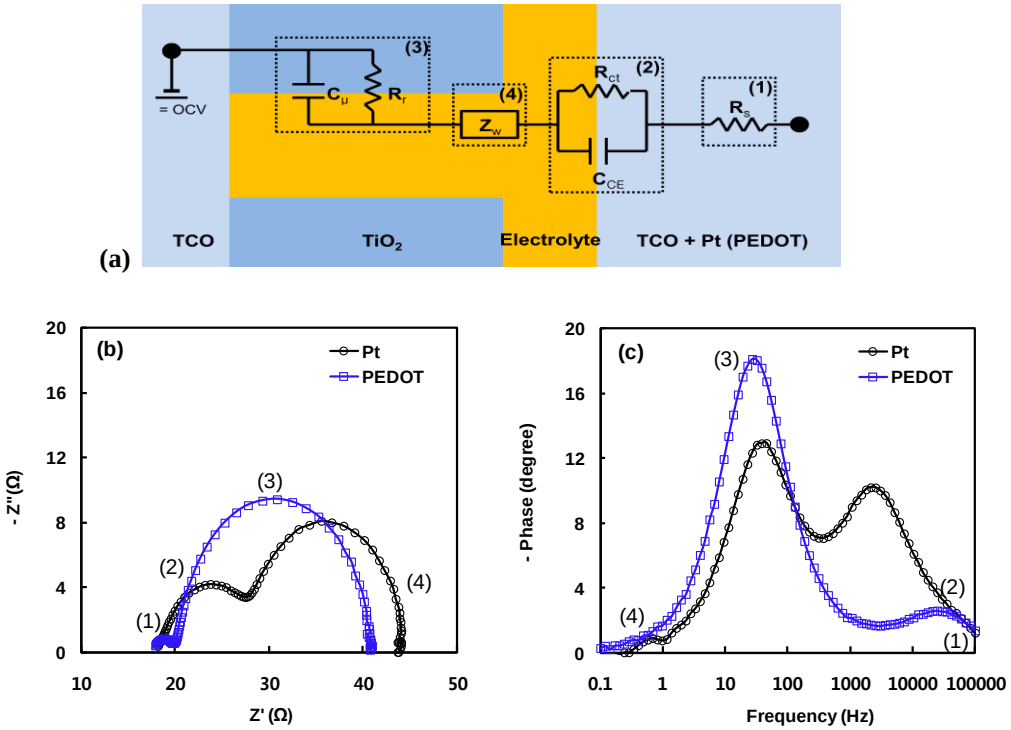


**Figure 5.** (a) The equivalent circuit for DSSC, (b) the Nyquist plots and (c) Bold plots of symmetric cells of platinum and PEDOT.

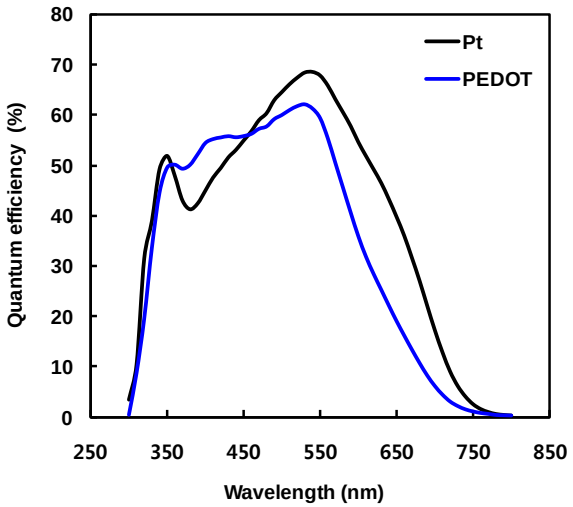


**Figure 6.** Incident photon to current conversion efficiencies of the DSSC using Pt and PEDOT counter electrode.

The IPCE values of the DSSC with the Pt and PEDOT CEs as a function of the illumination wavelength are shown in Figure 6. IPCE of PEDOT CE showed higher quantum efficiency in the wavelength of 450~800 nm than that of Pt CE. The PEDOT CE reaches a maximum IPCE of 70% at the wavelength of 540 nm while the Pt CE illustrates an IPCE of 60 %. The comparable photocurrent

and photovoltaic obtained using the PEDOT CE to the Pt-based CE are attributed to the increased effective surface area and good catalytic effect of PEDOT for $I_3^-$ reduction.

Figure 7 shows the *J–V* (Ed- this acronym has already been defined above) curves obtained for the DSSCs with different CEs. The photovoltaic parameters such as open-circuit voltage ($V_{OC}$), fill factor (*FF*), short-circuit current density ($J_{SC}$) and IPCE of the DSSCs were determined from these curves and are shown in Table 1. The DSSC with a PEDOT CE had the highest *Voc* and *FF*, with a good IPCE of 5.1%, in comparison to 5.2% obtained for the cell prepared with the Pt electrode. The 3-cycle PEDOT film exhibited a good *Voc* value due to its higher surface roughness and conductivity. (Ed- there is no respective comparison here) The *FF* and *Voc* values increased due to the reduced IR drops of the devices with the improved electrocatalytic activity and better adhesion of the PEDOT films on substrates.

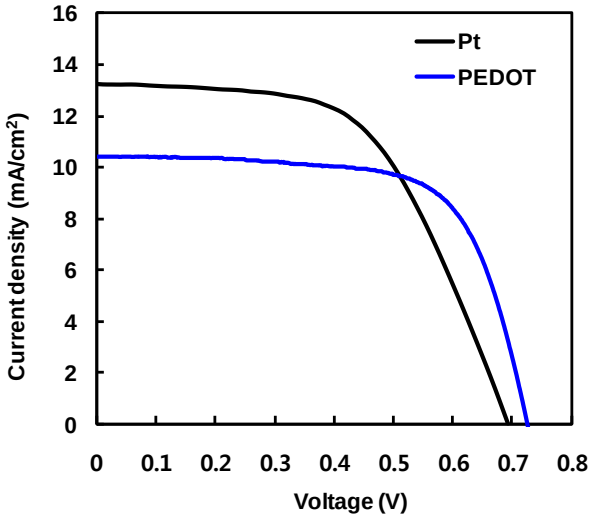


**Figure 7.** Photocurrent-voltage characteristics of the DSSCs using Pt and PEDOT counter electrode. The photovoltaic parameters are summarized in Table 1.

**Table 1.** Photovoltaic parameters of DSSCs based on Pt and PEDOT counter electrodes

| CE | $J_{SC}$ [mA/cm$^2$] | $V_{OC}$ [V] | *FF* | $\eta$ [%] | $R_{ct}(\Omega)$ |
|---|---|---|---|---|---|
| Pt | 13.2 | 0.69 | 0.57 | 5.2 | 10.2 |
| PEDOT | 10.4 | 0.73 | 0.68 | 5.1 | 2.3 |

## 4. CONCLUSIONS

PEDOT films were synthesized on FTO substrate by electro-oxidative polymerization using EDOT at room temperature. The PEDOT CE presented a higher catalytic effect with $I^-/I_3^-$ redox than did the Pt electrode. The DSSCs fabricated using these PEDOT films as the CE exhibited an efficiency

of 5.1%, which is almost equivalent to that of the standard Pt CE (5.2%). This improved PEDOT cell performance was attributed to the enhanced film active area and the reduced film charge-transfer resistance, as revealed by the CV and EIS results, respectively. Compared to the standard Pt CE, the PEDOT-based CE demonstrated promising and cost effective potential for application to DSSCs.

ACKNOWLEDGEMENTS
This research was supported by the Basic Science Research Program through the National Research Foundation of Korea (NRF), funded by the Ministry of Science, ICT and Future Planning (2012R1A1A3010655).

## References

1. M. Gratzel, *Prog. Photovolt. Res. Appl.*, 8 **(**2000) 171.
2. A. Hagfeldt, G. Boschloo, L. Sun, L Kloo and H. Pettersson, *Chem. Rev.*, 110 **(**2010) 6595.
3. Z. Ning, Y. Fu and H. Tian, *Energy Environ. Sci.*, 3 **(**2010) 1170.
4. L.L. Li, C.W. Chang, H.H. Wu, J.W. Shiu, P.T. Wu and E.W. Diau, *J. Mater. Chem.*, 22 **(**2012) 6267.
5. O.K. Varghese, M. Paulose and C.A. Grimes, *Nat. Nanotechnol.*, 4 **(**2009) 592.
6. Y. Saito, W. Kubo, T. Kitamura, Y. Wada and S. Yanagida, *J. Photochem. Photobiol. A*, 164 **(**2004) 153.
7. B. Fan, X. Mei, K. Sun and J. Ouyang, *Appl. Phys. Lett.*, 93 (2008) 143103.
8. X. Zhao, M. Li, D. Song, P. Cui, Z. Zhang, Y. Zhao, X. Shen and Z. Zhang, *Nanoscale Res. Lett.*, 9 (2014) 202.
9. K.H.Park, S.J. Kim, R. Gomes and A. Bhaumik, Chem. Eng. J., 260 (2015) 393.
10. S.H. Cho, S.H. Hwang, C.H. Kim and J.S. Jang, *J. Mater. Chem.*, 22 **(**2012) 12164.
11. G. Boschloo and A. Hagfeldt, *Accounts of Chem. Res.*, 42 **(**2009) 1819.
12. J.M. Pringle, V. Armel and D.R. MacFarlane, *Chem. Commun.*, 46 **(**2010) 5367.
13. S. Vivekaphirat, C. Saekung, S.H. Thang, A. Wongchaisuwat and M. Arunchaiya, *Materials Science Forum*, 663-665 **(**2010) 852.
14. F.J. Lim, K. Ananthanarayanan, J. Luther and G.W. Ho, *J. Mater. Chem.*, 22 **(**2012) 25057.
15. H.C. Ko, S.A. Park and H.S. Lee, *Synth. Met.*, 143 **(**2004) 31.
16. S.V. Selvaganesh, J. Mathiyarasu, K.L.N. Phani and V. Yegnaraman, *Nanoscale Res. Lett.*, 2 **(**2007) 546.
17. T.H. Lee, K.S. Do, Y.W. Lee, S.S. Jeon, C.W. Kim, J.J. Ko and S.S. Im, *J. Mater. Chem.*, 22 **(**2012) 21624.